1854

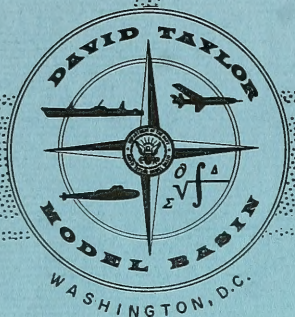

DEPARTMENT OF THE NAVY

DATA LIBRARY
Woods Hole Oceanographic Institution

HYDROMECHANICS

O

AERODYNAMICS

O

STRUCTURAL MECHANICS

O

APPLIED MATHEMATICS

O

ACOUSTICS AND TION

TESTS OF MACHINED HIGH-STRENGTH STEEL SPHERICAL SHELLS SUBJECTED TO EXTERNAL HYDROSTATIC PRESSURE

by

Albert E. Dadley

STRUCTURAL MECHANICS LABORATORY

RESEARCH AND DEVELOPMENT REPORT

August 1964 Report 1854

GC
.1
.D3
no.1854

DEMCO

MBL/WHOI
0 3001 0037644 4

TESTS OF MACHINED HIGH-STRENGTH STEEL SPHERICAL SHELLS SUBJECTED TO EXTERNAL HYDROSTATIC PRESSURE

by

Albert E. Dadley

August 1964

Report 1854
S-F013 03 02

TABLE OF CONTENTS

	Page
ABSTRACT	1
INTRODUCTION	1
DESCRIPTION OF MODELS	2
TEST PROCEDURE AND RESULTS	4
DISCUSSION OF RESULTS	5
CONCLUSIONS	8
ACKNOWLEDGMENTS	9
REFERENCES	20

LIST OF FIGURES

	Page
Figure 1 - Typical Compressive Stress-Strain Curves for Material (STS-Steel) Used in Machined Steel Models	10
Figure 2 - Representative Material Characteristics	10
Figure 3 - Details of the Cylinder-Spherical Boundary Intersections of the Models	11
Figure 4 - Collapsed Models	12
Figure 5 - Pressure versus Measured Change in Internal Volume for Model 7A	13
Figure 6 - Nondimensional Plot of Experimental Results for Machined Near-Perfect STS Hemispherical Shells	14

LIST OF TABLES

	Page
Table 1 - Model Dimensions	15
Table 2 - Measured Wall Thicknesses and Initial Departures from Sphericity	16
Table 3 - Pressures at Which Strains were Recorded	17
Table 4 - Measured Strain Sensitivity Coefficients	18
Table 5 - Comparison of Experimental Collapse Pressures with Theory for Near-Perfect Thin Spherical Shells	19

ABSTRACT

Six structural models, consisting of hemispherical shells bounded by ring-stiffened cylinders designed to provide ideal boundary conditions, were hydrostatically pressure-tested to collapse. The models were accurately machined from high-strength steel (STS) and were designed to investigate both elastic and inelastic buckling modes of collapse. The results of the tests are compared with theory, and the collapse pressures agree within ± 7 percent of those computed by the TMB empirical buckling equation.

A nondimensional plot of experimental results is presented for the models tested. Based on the plot, a simple design method is given for similar accurately machined thin spherical shells.

INTRODUCTION

In the past decade, increasing emphasis has been placed on the use of spherical shells in pressure vessels. Their use encompasses a wide range of applications for confinement of internal pressure, and there is an accelerating trend for external pressure applications in the field of deep underwater research.

Because most of the materials used in deep-sea underwater vehicles exhibit strain-hardening properties, which may deviate widely from the perfectly plastic (plateau) stress-strain pattern, there is a great need for wider understanding of the nature of inelastic buckling. However, greater knowledge of elastic buckling must also be emphasized in view of the growing interest in new tough materials such as glass and ceramics which have such extremely high compressive strengths that practical structural designs for pressure vessels prevent inception of yielding at even the greatest of ocean depths.[1] A historical background of the elastic and inelastic theories which apply to spherical shells subjected to external pressure has been extensively summarized in Reference 2.

To evaluate the validity of the hydrostatic collapse pressures predicted by the buckling formulas developed from the various spherical

---

[1]References are listed on page 20.

shell theories, six small accurately machined high-yield steel models were fabricated. To facilitate fabrication and subsequent instrumentation and thereby save time and funds, the models were designed and machined as hemispherical heads bounded by externally ring-stiffened reinforced cylinders in lieu of the actual spheres. The cylinder of each separate model was so designed as to simulate at the boundary the action of the remaining half of the sphere, i.e., membrane deflection and no rotation. The measured uniform strain-gage readings and collapse pressures are consistent with similar work being performed on spherical shells and suggest an adherence of the test results to the ideal boundary design.

Five of the models were designed to fail after the inception of yielding (inelastic buckling), and the remaining model was designed to fail well below the yield point within the elastic range (elastic buckling). The test results of these six near-perfect machined models, all of which failed within their proper ranges of elasticity, are presented in this report and compared with theory.

A nondimensional plot of experimental results is also presented and discussed. The plot is presented for the purpose of providing a simple method of structural design for similar accurately machined thin spherical shells with similar stress-strain patterns. The results of a similar plot currently being developed at the Model Basin from work performed on larger segmentally welded high-strength steel hemispherical shells are also discussed.

DESCRIPTION OF MODELS

Six hemispherical models bounded by external ring-stiffened cylinders were machined from high-strength, special-treatment steel (STS). Models 6, 4A, 4A Revised, 1CR, and 1CR Revised are approximately 7 in. in diameter and possess respective measured spherical shell thickness to nominal radius ratios (h/R) of 0.007, 0.017, 0.018, 0.035, and 0.036. Model 7A is approximately 4 in. in diameter and possesses an h/R equal to 0.003. Structural dimensions including the average compressive yield strengths as individually measured from eight representative sample coupons taken from the stock material of each model are presented in Table 1 together with a generalized sketch of the models. Typical stress-strain curves for the STS

plate used for the fabrication of each of the models are illustrated in Figure 1.

Figure 2 shows the representative ratios of the square root of the multiplicand of the secant and tangent modulii to the elastic modulus as a function of uniaxial compressive stress for the curves of the inelastic models of Figure 1. These curves describe the plastic behavior of the material and were used in the calculations to obtain the Taylor Model Basin (TMB) inelastic buckling pressures P_E presented indirectly later in this report.

All the models, with the exception of Model 7A, were machined identically. First, the inside contour was machined using a form tool, then the outside contour was machined using a lathe and ball-turning attachment, and finally, the exterior ring-stiffened cylinder was machined.[3] Model 7A, the last model fabricated, was machined more accurately using a method similar to that just mentioned but with the addition of a more recently developed system consisting of a support pot and mating mandrel.[4]

All the models were designed for membrane deflection and no rotation at the intersections of the hemispheres and the cylinders. By maintaining lower stresses in the cylindrical than in the spherical portion of the model and thereby assuring failure in the area of interest, this design prevents the boundary with the cylinder from altering the stress pattern in the hemisphere from the pattern that would be created in a sphere of the same material, radius, and shell thickness. The inside diameters of the cylinders of Models 4A and 1CR were designed to be slightly smaller than those of the hemispheres for Model 1CR (Figure 3a).

Because of machining error, the cylindrical portion of Model 4A was fabricated with a slight overcut; see Figure 3b. Although this resulted in a thinning of the cylindrical shell, thereby varying the ideal boundary condition somewhat, the spherical shell was machined correctly. Figure 3c illustrates the structural boundary configuration for Models 6 and 7A and also for the revised design of Models 4A and 1CR, all of which were fabricated with equal cylindrical and spherical radii.

Model 6 was accidentally machined with a small gouge around the outer circumference of the third frame from the boundary juncture. As a result, approximately 16 percent of the area of the frame was removed,

having a possible adverse effect on the ideal design of membrane deflection and no rotation of the juncture.

Table 2 lists the measured spherical wall thicknesses for the hemispheres of all the models. Table 2 also indicates the initial departures from sphericity for the hemispheres of Models 4A Revised, 1CR Revised, and 7A. Because the importance of sphericity measurements had not been established at the beginning of the tests, they were not taken on the three models tested earlier. All the thickness measurements were taken using a vidigage, and the initial sphericity departures were measured from a fixed point using a dial gage in a jig-bore.[4]

TEST PROCEDURE AND RESULTS

Each model was instrumented with strain gages in both the meridional and circumferential directions of the spherical portions with 1/8- and 1/16-in.-long foil-backed strain gages. The gages were placed in the configuration indicated in Table 2 to obtain strain distributions along the hemisphere toward the intersection with the cylinder. Strain gages could not be located at the boundary of the sphere and the cylinder because of the lack of clearance at the frame at this location. However, gages were located as close to this intersection as was physically possible.

All models were tested using oil as an external pressure medium. The models were externally loaded in comparatively small pressure tanks to limit destruction after collapse. Model 1CR Revised, however, which failed at a relatively high pressure, was quite severely damaged.

Pressure was applied incrementally to each model as indicated in Table 3. Before the strains were read at each increment of load, pressure was maintained for 3 min to allow the stresses in the model to stabilize. The experimental strain-sensitivity coefficients, i.e., the slopes of the pressure-strain plots in inch per inch per pounds per square inch for each strain gage are presented in Table 4. Table 5 lists the collapse pressures of the six models. Photographs of collapsed Models 4A Revised, 1CR Revised, and 7A are shown in Figure 4.

The pressure-strain plots for Model 7A, the only model designed to fail within the elastic range, properly displayed no significant nonlinear strain behavior for any of the loading cycles. Figure 5 is a plot of

pressure versus change in internal volume for the final pressure loading of Model 7A; the insignificant variation from linearity of the curve indicates the elastic behavior of the model up to its collapse.

DISCUSSION OF RESULTS

Collapse pressures of the six models tested are compared with the previous work of Zoelly and Timoshenko,[5] Bijlaard,[6] and Krenzke[3] in Table 5. The theoretical collapse pressures were computed using a Young's modulus of 30×10^6 psi, and a Poisson's ratio of 0.3 in the elastic range and 0.5 in the plastic range.

The theoretical collapse pressures of those models designed to fail in the inelastic range are presented in Table 5. Experimental collapse pressures are within 7 percent ($P_{EXP}/P_E = 0.93$) of the pressures of the empirical inelastic collapse formula developed at the Model Basin.[3] As expected, these results are consistent with those obtained by Krenzke[3] for aluminum models fabricated in a similar manner. The inelastic collapse pressures of Bijlaard also appear consistent with those inelastic values of Krenzke, indicating theoretical collapse pressures that are somewhat larger in every case than the respective theoretical collapse pressures calculated by the TMB empirical inelastic formula.

Comparison of the membrane strain sensitivities for Models 4A Revised, 1CR Revised, and 7A obtained at the 2-deg longitudinal locations with those obtained at the remaining longitudinal locations reveals only small variations in membrane deflections. Comparison of the inside and the outside strain sensitivities in the longitudinal direction at the juncture of the hemisphere with the cylinder does indicate varying degrees of bending. As listed in Table 2, the smaller values of spherical thickness for each model obtained at the 2-deg locations as compared with the other locations suggest a reason for such bending. All sphericity deviations, also listed in Table 2, were very small, indicating insignificant variations from nominal radii. In light of the satisfactory results obtained, the deflection and rotation at the boundary of the cylinder and the hemisphere appear to have been adequately considered. As indicated in Table 5, the maximum deviation between experimental collapse pressure and that computed from the TMB empirical inelastic equation was 7 percent

(Model 6). It is possible that a premature failure occurred as a result of the machining error in the third frame of the model. The irregularity may have created a weakness in the hemisphere due to an increase in stress set up by a deviation in the desired boundary condition. The strain-sensitivity coefficients shown in Table 4 at the 2-deg longitudinal locations for Model 6 indicate greater membrane deflection than at any other location on the hemisphere. It is possible that analogous action resulted from the pressure loading of Model 4A due to the overcutting of the inside of the cylinder wall; a discrepancy in the desired boundary condition in this model may have effected a similar decrease in its collapse pressure.

The elastically designed Model 7A developed a collapse pressure of 290 psi. This is approximately 74 percent of the classical theoretical value of Zoelly and Timoshenko and 107 percent of the empirical elastic value of Krenzke.

The theoretical values of pressures presented in this report were calculated using the nominal values of the radius and the thinnest measured values of the spherical thickness taken for each model. As indicated by the ratios of experimental collapse pressure to the TMB empirical buckling collapse pressure P_E in Table 5, results for all the models showed reasonable agreement over a wide range of ratios of hemisphere thickness to radius. This consistency may be attributed to the high standard of precision maintained in the machining process. Since the models were not stress relieved, residual machining stresses were present, but they are considered negligible in view of the very small sphericity departures indicated in Table 2. The good correlation of experimental to theoretical collapse value obtained for Model 7A (to which the most rigorous conditions were adhered in the machining process) tends to support the suggestion of Reference 4 that if machining standards could be maintained sufficiently high to satisfy the rigid assumptions of classical buckling theory, then the classical formula could be used for thin spherical shell design. However, even if such high quality control could be obtained, cost and time requirements would undoubtedly be prohibitive for prototype construction.

The experimental results for the models pertaining to this report are plotted nondimensionally in Figure 6. The ordinate is the ratio of experimental collapse pressure to the equilibrium yield pressure P_y, as

defined in Table 5, and was obtained by applying a 0.2-percent strain offset as illustrated by the dotted lines in Figure 1. The abscissa is a ratio of the TMB empirical theoretical elastic buckling pressure P_3 to the same equilibrium yield pressure. The points display over a wide range of elastic stability, defined as the ratio of P_3 to P_y, the proximity of the test results to an idealized plot of a perfectly plastic (plateau) stress-strain curve indicated by the solid line in Figure 6.

The value of the comparison is to indicate that for accurately machined spherical shells with similar stress-strain curves, the results define an empirical curve (dotted line in Figure 6) which departs from the elastic portion of the ideal curve at some arbitrary elastic stability ratio and rejoins the plateau of the ideal curve at some higher arbitrary elastic stability ratio.

The purpose of obtaining such an empirical plot is to establish for any thin spherical shell design a practical design curve from which a single design formula can be selected. By knowing the design values of shell radius, material compressive stress as determined from test coupons, and required collapse pressure, an approximate elastic stability ratio can be calculated. If the ratio were to fall on the elastic portion of the ideal curve, the shell would be designed using the TMB empirical elastic equation; if on the plateau of the ideal curve, the shell would be designed using the simple equilibrium yield pressure formula P_y; and if the ratio were to fall on the empirical portion of the curve, then the shell could be designed by method of trial and error, using the reduced value of P_{EXP}/P_y found on the ordinate of the empirical curve.

By using any other selected empirical pressure formula, an empirical curve similar to that in Figure 6 could be derived to gain the same practical end. A similar curve is currently being developed as a part of the Model Basin hemispherical head program for high-strength steel models.[7] The models of Reference 7, however, are of a larger scale (approximately 3 to 5 1/2 ft in diameter) and are not machined but are fabricated by welding, resulting in a similar, yet individual curve to the one presented in this report. Each of the fabricated models of Reference 7 is constructed of pressed segmented sections, resulting in bending due to misalignment and sizeable residual stresses due to welding, undoubtedly

affecting the collapse pressure and consequently nondimensional curve plots, to some degree. Also, due to the impracticability of constructing separate cylinders for each of the models of Reference 7, a single cylinder is used for all. As a result, none of the models is designed with the ideal boundary conditions of membrane deflection and no rotation, thereby further altering the stress pattern in the fabricated spherical shells.

It should be emphasized that the plotted portion in Figure 6 should not be used for design purposes at this time because data are insufficient to verify its accuracy. Under no circumstances should the curve be used for design purposes unless the proposed spherical shell is to be designed and fabricated with the same accuracy as those models presented in this report; this precludes all but near-perfect machined models with ideal boundary conditions (where applicable). The curve may be used to design a spherical shell of any material provided it has the same shape stress-strain curve as those for inelastic failure design illustrated in Figure 1.

CONCLUSIONS

1. The experimental collapse pressures agree within ± 7 percent of the theoretical buckling pressures obtained from the inelastic empirical buckling formula for spherical shells developed at the Model Basin.

2. The experimental collapse pressures of Models 6 and 4A may be misleadingly low because of slight deviations from design due to errors in fabrication which occurred during the process of machining.

3. The design of ideal boundary (membrane deflection and no rotation) at the juncture of the hemisphere with the cylinder appears effective in preventing the cylinder from altering the stress pattern (and consequently the collapse pressure) in the hemisphere from the pattern that would be created in a sphere of the same material, radius, and shell thickness.

4. The empirical portion of the nondimensional plot of results for machined high-strength steel hemispherical shells (Figure 6) should not be used for design purposes pending verification of its accuracy.

5. Upon verification of the accuracy of the empirical portion of the curve of Figure 6, it may be used for design purposes only when the proposed spherical shell is fabricated with the same accuracy as the

models of this report and provided the stress-strain curve of the material used has the same shape as those for inelastic failure design illustrated in Figure 1.

ACKNOWLEDGMENTS

The author acknowledges the technical assistance of Messrs. Martin A. Krenzke and Robert F. Keefe and the contribution of Mr. Pendleton E. Humphries who conducted the hydrostatic tests.

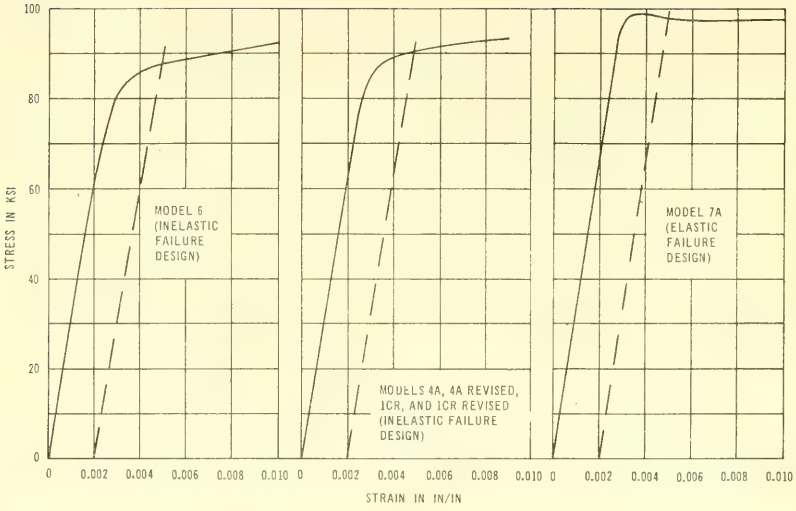

Figure 1 - Typical Compressive Stress-Strain Curves for Material (STS-Steel) Used in Machined Steel Models

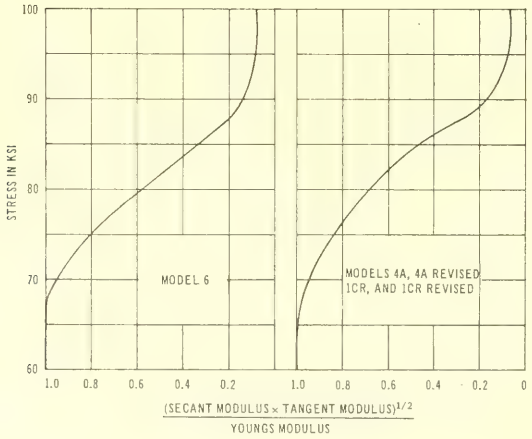

Figure 2 - Representative Material Characteristics

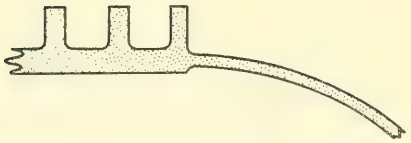

Figure 3a - Model 1CR

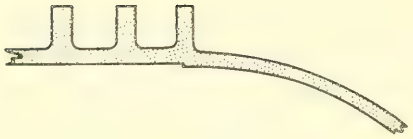

Figure 3b - Model 4A

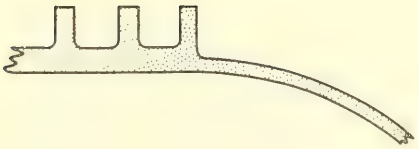

Figure 3c - Models 6, 4A Revised,
1CR Revised, and 7A

Figure 3 - Details of the Cylinder-Spherical Boundary Intersections of the Models

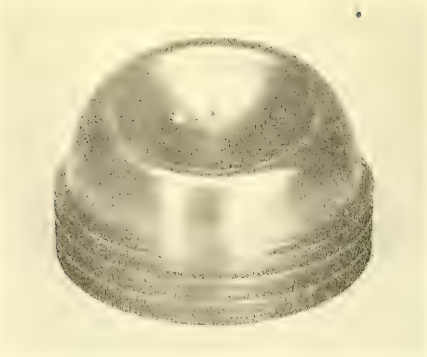

Figure 4a - Model 4A Revised

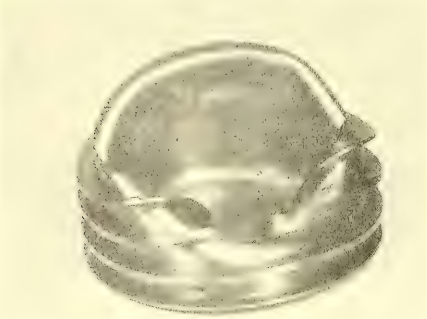

Figure 4b - Model 1CR Revised

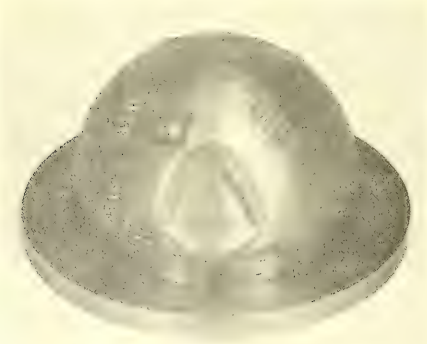

Figure 4c - Model 7A

Figure 4 - Collapsed Models

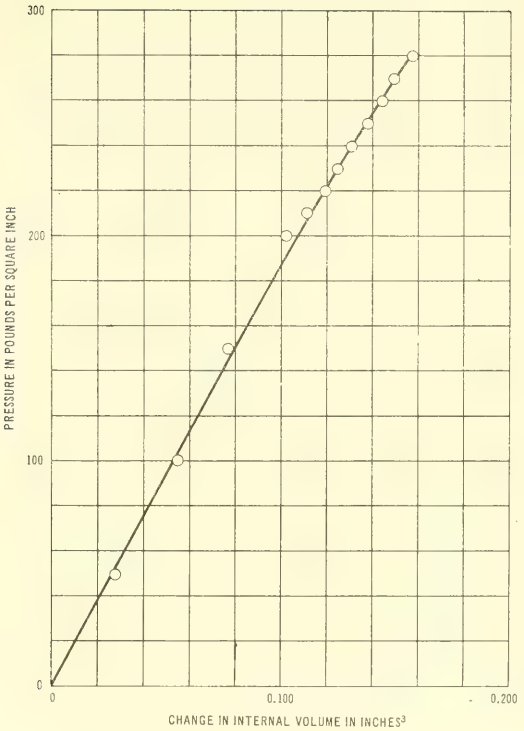

Figure 5 - Pressure versus Measured Change in Internal Volume for Model 7A

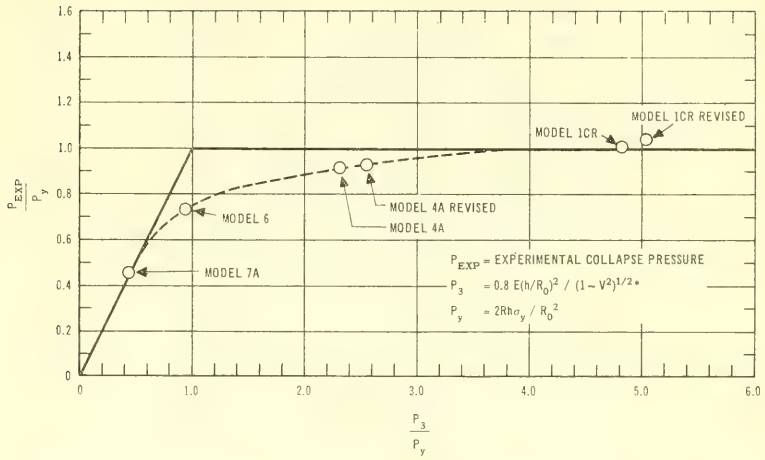

Figure 6 - Nondimensional Plot of Experimental Results for Machined Near-Perfect STS Hemispherical Shells

*P_3 is empirical elastic buckling pressure for spherical shells developed from recent TMB tests and P_y is equilibrium yield pressure where h is shell thickness, R is mean radius, R_0 is outer radius, E is Young's modulus, ν is Poisson's ratio, and σ_y is average material yield stress.

TABLE 1

Model Dimensions

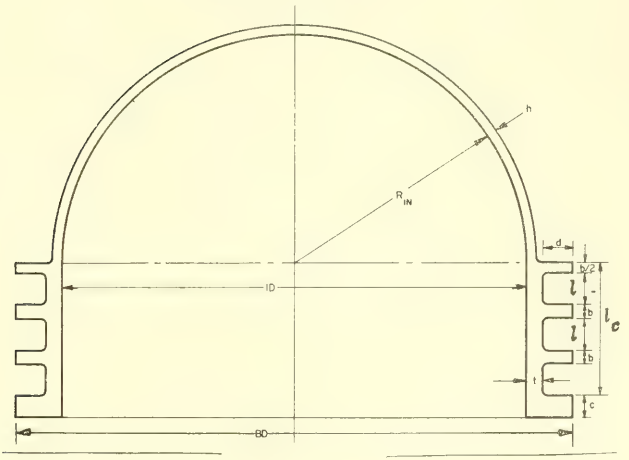

Model Number	Average Compressive Yield Strength	Structural Dimensions in inches										
		Spherical Wall Thickness h*	Nominal Inside Spherical Radius R_{in}	Inside Cylinder Diameter ID	Cylinder Wall Thickness t	Frame Thickness b	Frame Depth d	Bay Length l	Cylinder Length l_c	Model Base Flange Thickness c	Outside Base Diameter BD	Number of Cylinder Bays
	psi	in.	in.	in.	in.	in.	in.	in.	in.	in.	in.	
6	92,000	0.0275	3.975	7.949	0.051	0.044	0.091	0.316	1.057	0.022	8.233	3
4A	90,770	0.064	3.812	7.646	0.107	0.138	0.299	0.516	1.892	0.069	8.440	3
4A Revised	90,770	0.071	3.825	7.652	0.118	0.131	0.264	0.480	1.769	0.066	8.411	3
1CR	90,770	0.113	3.190	6.312	0.200	0.226	0.420	0.619	2.423	0.111	7.552	3
1CR Revised	90,770	0.118	3.190	6.380	0.199	0.204	0.406	0.571	2.222	0.102	7.590	3
7A	96,120	0.0066	2.0065	4.013	0.0073	0.035	0.027	0.071	0.407	0.380	5.500	4

*Smallest measured value is listed for h.

TABLE 2

Measured Wall Thicknesses and Initial Departures from Sphericity

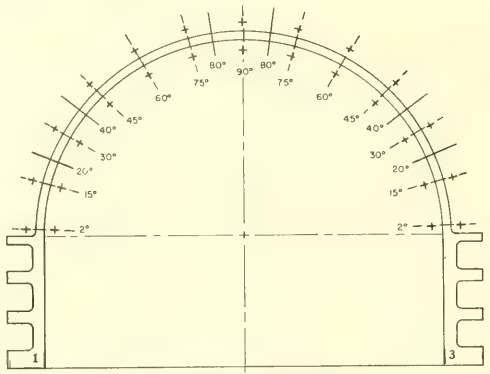

CIRCUMFERENTIAL ORIENTATION

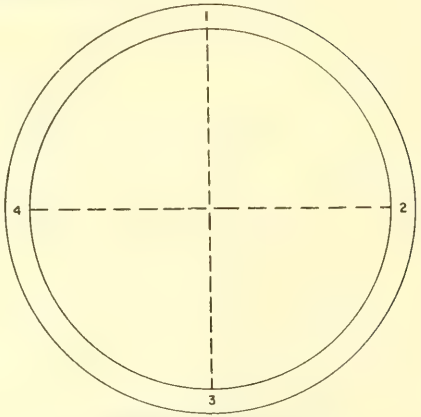

MERIDIONAL ORIENTATION

Model Number	Meridional Orientation	Spherical Wall Thickness in Inches — Circumferential Orientation in Degrees from Base of Hemisphere										Departure from Nominal Outer Radius in Inches* — Circumferential Orientation in Degrees from Base of Hemisphere									
		2	15	20	30	40	45	60	75	80	90	2	15	20	30	40	45	60	75	80	90
6	1			0.030		0.030		0.028		0.028	0.028										
4A	1			0.069		0.069		0.068		0.065	0.064										
ICR	1	0.117	0.119		0.120		0.118	0.119	0.113		0.115										
4A Revised	1	0.073		0.077		0.076		0.072		0.071	0.071	0		-0.0004		-0.0011		-0.0013		-0.0011	0
	2	0.073		0.077		0.076		0.073		0.071		0		-0.0002		-0.0008		-0.0012		-0.0011	
	3	0.073		0.077		0.076		0.073		0.071		0		-0.0005		-0.0011		-0.0015		-0.0010	
	4	0.073		0.076		0.076		0.072		0.071		-0.0001		-0.0004		-0.0010		-0.0014		-0.0010	
ICR Revised	1	0.123		0.123		0.123		0.122		0.120	0.118	0		-0.0018		-0.0010		0		+0.0001	0
	2	0.124		0.124		0.124		0.122		0.121		0		-0.0011		-0.0009		0		0	
	3	0.124		0.124		0.123		0.122		0.121		0		-0.0007		-0.0005		+0.0003		+0.0002	
	4	0.124		0.124		0.124		0.122		0.121		-0.0002		-0.0017		-0.0011		+0.0001		0	
7A	1	0.0066			0.0070			0.0075			0.0072	0	-0.0002		-0.0005		-0.0006	-0.0009	-0.0003		0
	2	0.0066			0.0070			0.0074				0	-0.0002		-0.0004		-0.0005	-0.0008	-0.0003		
	3	0.0066			0.0070			0.0073				0	-0.0003		-0.0005		-0.0007	-0.0009	-0.0003		
	4	0.0066			0.0070			0.0073				0	-0.0005		-0.0005		-0.0008	-0.0009	-0.0003		

*Minus sign (-) designates inward departure.

Note: Crossed lines (+) on model profile sketch represent strain gage locations.

TABLE 3

Pressures at Which Strains were Recorded

Pressure psi	Model 6		Pressure psi	Model 4A			Model 4A Revised			Pressure psi	Model 1CR		Model 1CR Revised			Pressure psi	Model 7A		
	Run 1	Run 2		Run 1	Run 2	Run 3	Run 1	Run 2	Run 3		Run 1	Run 2	Run 1	Run 2	Run 3		Run 1	Run 2	Run 3
0	x	x	0	x	x	x	x	x	x	0	x	x	x	x	x	0	x	x	x
100	x		200	x			x			500	x		x			10	x		
200	x	x	400	x			x			1000	x	x	x	x		20	x		
300	x		500		x			x		1500	x		x			25		x	
400	x	x	600	x			x			2000	x	x	x	x	x	30	x		
500	x	x	800	x			x			2500	x		x			40	x		
600	x	x	1000	x	x	x	x	x	x	2750	x					50	x	x	x
700		x	1200	x	x		x	x		3000	x	x	x	x		60	x		
800		x	1400		x			x		3250	x					70	x		
850		x	1500		x	x		x	x	3500	x			x		75		x	
875		x	1600		x			x		3750	x					80	x		
900		x	1700		x			x		4000	x	x		x	x	90	x		
925		*	1800		x			x		4200	x					100	x	x	x
0	x	x	1900		x			x		4400	x					110		x	
			2000		x	x		x	x	4500		x		x		120		x	
			2100			x			x	4600	x					130		x	
			2200			x			x	4750		x				140		x	
			2300			x			x	4800	x					150		x	x
			2350			x			x	5000	x	x		x	x	160		x	
			2400			x			x	5200		x				170		x	
			2450			x			x	5400		x				180		x	
			2500			x			x	5500		x			x	190		x	
			2550			x			x	5600		x				200		x	x
			2600			x			x	5700		x				210			x
			2650			x			x	5800		x				220			x
			2700			**			x	5900		x				230			x
			2750						x	6000		x			x	240			x
			2800						x	6050		x				250			x
			2850						x	6100		x				260			x
			2900						x	6160		*				270			x
			2950						x	6200					x	280			x
			3000						x	6400					x	290			*
			3050						x	6500					x	140		x	
			3060						*	6600					**	70		x	
			0	x	x		x	x	x	0	x		x	x	x	0	x	x	x

*Model failure, no reading taken.

**Model failure, strain readings obtained.

TABLE 4

Measured Strain Sensitivity Coefficients*

Longitudinal Location on Membrane	Location		Model 4A				Model 6				Model 1CR			
			Inside		Outside		Inside		Outside		Inside		Outside	
	Meridional Orientation		1	2	3	2	1	3	1	1	1	2	3	2
90 deg.	ϵ_x		-0.71		-0.41		+2.04		+1.91		-0.17		-0.34	
	ϵ_y		-0.74		-0.71		-3.76		-2.10		-0.14		-0.31	
45 deg.	ϵ_x													
	ϵ_y													
60 deg.	ϵ_x			-0.77		-0.74	+1.74	-1.69	+1.40	+1.85	-0.15		-0.12	
	ϵ_y			-0.76		-0.71	+1.74	+1.40	-1.42	+1.74	-0.16		-0.13	
45 deg.	ϵ_x		-0.64		-0.69							-0.35		-0.11
	ϵ_y		-0.73		-0.69							-0.35		-0.11
30 deg.	ϵ_x			-0.7.		-0.67	-1.56	+1.53	-1.66	+1.62	-0.13		-0.11	
	ϵ_y			-0.7.		-0.64	+1.49	-1.47	+1.62	-1.69	-0.16		out	
0 deg.	ϵ_x													
	ϵ_y													
2 deg.	ϵ_x							-0.21		-2.64				
	ϵ_y							-2.47		-2.61				

Longitudinal Location on Membrane	Location		Model 4A Revised								Model 1CR Revised							
			Inside				Outside				Inside				Outside			
	Meridional Orientation		1	2	3	4	1	2	3	4	1	2	3	4	1	2	3	4
90 deg.	ϵ_x			-0.71				-0.62				-0.44				-0.32		
	ϵ_y			-0.69				-0.64				-0.37				-0.32		
45 deg.	ϵ_x				-0.67				-0.64				-0.35				-0.32	
	ϵ_y				-0.68				-0.64				-0.35				-0.32	
60 deg.	ϵ_x		-0.69			-0.64	-0.61			-0.61	-0.34			-0.34	-0.32			-0.32
	ϵ_y		-0.68			-0.64	-0.61			-0.64	-0.35			-0.32	-0.32			
45 deg.	ϵ_x		-0.66		-0.69		-0.62		-0.62		-0.34		-0.34		-0.32		-0.32	
	ϵ_y		-0.65		-0.66		-0.62		-0.62		-0.34		-0.33		-0.32		-0.32	
30 deg.	ϵ_x		-0.67		-0.67		-0.58		-0.60		-0.31		-0.27		-0.33		-0.32	
	ϵ_y		out		-0.65		-0.60		-0.63		-0.34		-0.32		-0.31		-0.31	
0 deg.	ϵ_x			-0.69		-0.69		-0.57		-0.56		-0.34		-0.33		-0.29		-0.24
	ϵ_y			-0.67		-0.65		-0.62		out		-0.35		-0.34		-0.33		-0.33
2 deg.	ϵ_x		-0.66	-0.69	-0.67	-0.62	-1.01	-0.86	-0.60	-0.89	-0.33	-0.29	-0.20	-0.25	-0.44	-0.39	out	out
	ϵ_y		-0.71	-0.66	-0.71	-0.72	-0.68	-0.66	-0.72	-0.69	-0.37	-0.30	-0.19	-0.36	-0.35	-0.34	out	-0.29

Longitudinal Location on Membrane	Location		Model 7A							
			Inside				Outside			
	Meridional Orientation		1	2	3	4	1	2	3	4
90 deg.	ϵ_x		-1.25				-1.35			
	ϵ_y		-3.05				-1.20			
45 deg.	ϵ_x									
	ϵ_y									
60 deg.	ϵ_x									
	ϵ_y									
45 deg.	ϵ_x		-1.25	-1.50	-1.20	-1.45	-1.20	-1.25	-1.10	-1.30
	ϵ_y		-1.45	-1.10	-1.20	-1.35	-1.05	-1.05	-1.05	-1.20
30 deg.	ϵ_x									
	ϵ_y									
0 deg.	ϵ_x									
	ϵ_y									
2 deg.	ϵ_x		-3.40	-3.40	-1.65	-1.50	-4.70	-4.75	-2.70	-1.50
	ϵ_y		-2.40	-3.30	-1.20	-1.25	-3.70	-1.55	-3.25	-3.00

*Values are listed in microinches per pounds per square inch with negative values representing compressive strain. Gage locations are represented on diagram of Table 2.

**ϵ_x Represents strain sensitivity measured in longitudinal direction, and

ϵ_y Represents strain sensitivity measured in meridional direction.

TABLE 5

Comparison of Experimental Collapse Pressures with Theory for Near-Perfect Thin Spherical Shells

Model	Experimental Collapse Pressure P_{EXP} *	$\frac{P_{EXP}}{P_1}$ **	$\frac{P_{EXP}}{P_3}$ †	$\frac{P_{EXP}}{P_y}$ ††	$\frac{P_{EXP}}{P_B}$ ‡	$\frac{P_{EXP}}{P_E}$ ‡‡	$\frac{P_3}{P_E}$
6	925	0.54	0.78	0.73	0.84	0.93	1.20
4A	2700	0.27	0.39	0.91	0.94	0.96	2.45
4A Revised	3060	0.25	0.37	0.93	0.95	0.98	2.68
1CR	6160	0.14	0.21	1.01	1.01	1.02	4.87
1CR Revised	6600	0.14	0.21	1.04	1.04	1.05	5.09
7A	290	0.74	1.07	0.46	0.74	1.07	1.00

* All pressure values are in psi,

** P_1 (Classical elastic linear buckling pressure of Zoelly and Timoshenko[5]) $= 1.21\ E(h/R)^2$

† P_3 (Empirical elastic buckling pressure for machined spherical shells developed from recent Model Basin tests[3]) $= 0.8\ E(h/R_o)^2 / (1 - \nu^2)^{1/2}$

†† P_y (Equilibrium yield pressure) $= 2Rh\ \sigma_y / R_o^2$

‡ P_B (Inelastic buckling pressure of Bijlaard[6]) $= 1.154\ [E_s E_t/(1 - \nu_p^2)]^{1/2}\ (h/R)^2$

‡‡ P_E (Empirical inelastic buckling pressure for machined spherical shells developed from recent Model Basin tests[3]) $= 0.8\ [E_s E_t / (1 - \nu^2)]^{1/2}\ (h/R_o)^2$

Where h = Spherical shell thickness
R = Mean spherical radius
R_o = Outer spherical radius
E = Young's modulus
E_s = Secant modulus
E_t = Tangent modulus
ν = Poisson's ratio in the elastic range
ν_p = Poisson's ratio in the plastic range
σ_y = Average material yield stress

REFERENCES

1. Krenzke, M. A., "Exploratory Tests of Long Glass Cylinders under External Hydrostatic Pressure," David Taylor Model Basin Report 1641 (Aug 1962).

2. Krenzke, M. A. and Kiernan, T. J., "Tests of Stiffened and Unstiffened Machined Spherical Shells under External Hydrostatic Pressure," David Taylor Model Basin Report 1741 (Aug 1963).

3. Krenzke, M. A., "Tests of Machined Deep Spherical Shells under External Hydrostatic Pressure," David Taylor Model Basin Report 1601 (May 1962).

4. Krenzke, M. A., "The Elastic Buckling Strength of Near-Perfect Deep Spherical Shells with Ideal Boundaries," David Taylor Model Basin Report 1713 (Jul 1963).

5. Timoshenko, S., "Theory of Elastic Stability," McGraw-Hill Book Co., Inc., New York (1936).

6. Bijlaard, P. P., "Theory and Tests in the Plastic Stability of Plates and Shells," Journal of the Aeronautical Sciences, Vol. 16, No. 9 (Sep 1949).

7. Kiernan, T. J., "The Buckling Strength of Segmented HY-80 Steel Hemispheres," David Taylor Model Basin Report 1721 (in preparation).

INITIAL DISTRIBUTION

Copies	
15	CHBUSHIPS 2 Sci & Res (Code 442) 1 Lab Mgt (Code 320) 3 Tech Lib (Code 210L) 1 Struc Mech, Hull Mat & Fab (Code 341A) 1 Prelim Des Br (Code 420) 1 Prelim Des Sec (Code 421) 1 Ship Protec (Code 423) 1 Hull Des Br (Code 440) 1 Struc Sec (Code 443) 2 Sub Br (Code 525) 1 Pres Ves Sec (Code 651F)
2	CHONR 1 Struc Mech Br (Code 439) 1 Undersea Programs (Code 466)
4	CNO 1 Plans, Programs & Req Br (Op 311) 1 Tech Anal & Adv Gr (Op 07T) 1 Sub Program Br (Op 713) 1 Tech Support Br (Op 725)
20	CDR, DDC
1	CO & DIR, USNMEL
1	CDR, USNOL
1	DIR, USNRL (Code 2027)
1	CO & DIR, USNUSL
1	CO & DIR, USNEL
1	CDR, USNOTS, China Lake
1	CDR, USNOTS, Pasadena
1	CO, USNUOS
2	NAVSHIPYD PTSMH
2	NAVSHIPYD MARE
1	NAVSHIPYD CHASN
1	SUPSHIP, Groton
1	EB DIV, Gen Dyn Corp
1	SUPSHIP, Newport News
1	NNSB & DD Co.

Copies	
1	SUPSHIP, Pascagoula
1	Ingalls Shipbldg Corp
1	SUPSHIP, Camden
1	New York Shipbldg
1	DIR DEF, R & E, Attn: Tech Lib
1	CO, USNROTC & NAVADMINU, MIT
1	O in C, PGSCOL, Webb
1	DIR, APL, Univ of Wash, Seattle
1	NAS, Attn: Comm on Undersea Warfare
1	Prof. J. Kempner, PIB
1	Dr. E. Wenk, Jr., The White House
1	Dr. R. DeHart, SWRI
1	Mr. Leonard P. Zick, Chicago Bridge & Iron Co.
1	Dean V. L. Salerno, Fairleigh Dickenson Univ.
1	Prof. E. O. Waters, Yale Univ
2	Mr. C. F. Larson, Sec, Welding Research Council
1	Prof. Bernard Budiansky, Harvard Univ
1	Mr. J. Mavor, WHOI

David Taylor Model Basin. Report 1854.
TESTS OF MACHINED HIGH-STRENGTH STEEL SPHERICAL SHELLS SUBJECTED TO EXTERNAL HYDROSTATIC PRESSURE, by Albert E. Dadley. Aug 1964. ii, 21p. illus., tables, graphs, refs. UNCLASSIFIED

Six structural models, consisting of hemispherical shells bounded by ring-stiffened cylinders designed to provide ideal boundary conditions, were hydrostatically pressure tested to collapse. The models were accurately machined from high-strength steel (STS), and were designed to investigate both elastic and inelastic buckling modes of collapse. The results of the tests are compared with the theory and the collapse pressures agree within ± 7 percent of those computed by the TMB empirical buckling equation.

1. Hemispherical shells (Stiffened)--Collapse--Model tests
2. Hemispherical shells (Stiffened)--Hydrostatic pressure
3. Submarine hulls--Structural analysis
4. Spherical shells (Stiffened)--Design
I. Dadley, Albert E.
II. S-F013 03 02

David Taylor Model Basin. Report 1854.
TESTS OF MACHINED HIGH-STRENGTH STEEL SPHERICAL SHELLS SUBJECTED TO EXTERNAL HYDROSTATIC PRESSURE, by Albert E. Dadley. Aug 1964. ii, 21p. illus., tables, graphs, refs. UNCLASSIFIED

Six structural models, consisting of hemispherical shells bounded by ring-stiffened cylinders designed to provide ideal boundary conditions, were hydrostatically pressure tested to collapse. The models were accurately machined from high-strength steel (STS), and were designed to investigate both elastic and inelastic buckling modes of collapse. The results of the tests are compared with the theory and the collapse pressures agree within ± 7 percent of those computed by the TMB empirical buckling equation.

1. Hemispherical shells (Stiffened)--Collapse--Model tests
2. Hemispherical shells (Stiffened)--Hydrostatic pressure
3. Submarine hulls--Structural analysis
4. Spherical shells (Stiffened)--Design
I. Dadley, Albert E.
II. S-F013 03 02

David Taylor Model Basin. Report 1854.
TESTS OF MACHINED HIGH-STRENGTH STEEL SPHERICAL SHELLS SUBJECTED TO EXTERNAL HYDROSTATIC PRESSURE, by Albert E. Dadley. Aug 1964. ii, 21p. illus., tables, graphs, refs. UNCLASSIFIED

Six structural models, consisting of hemispherical shells bounded by ring-stiffened cylinders designed to provide ideal boundary conditions, were hydrostatically pressure tested to collapse. The models were accurately machined from high-strength steel (STS), and were designed to investigate both elastic and inelastic buckling modes of collapse. The results of the tests are compared with the theory and the collapse pressures agree within ± 7 percent of those computed by the TMB empirical buckling equation.

1. Hemispherical shells (Stiffened)--Collapse--Model tests
2. Hemispherical shells (Stiffened)--Hydrostatic pressure
3. Submarine hulls--Structural analysis
4. Spherical shells (Stiffened)--Design
I. Dadley, Albert E.
II. S-F013 03 02

David Taylor Model Basin. Report 1854.
TESTS OF MACHINED HIGH-STRENGTH STEEL SPHERICAL SHELLS SUBJECTED TO EXTERNAL HYDROSTATIC PRESSURE, by Albert E. Dadley. Aug 1964. ii, 21p. illus., tables, graphs, refs. UNCLASSIFIED

Six structural models, consisting of hemispherical shells bounded by ring-stiffened cylinders designed to provide ideal boundary conditions, were hydrostatically pressure tested to collapse. The models were accurately machined from high-strength steel (STS), and were designed to investigate both elastic and inelastic buckling modes of collapse. The results of the tests are compared with the theory and the collapse pressures agree within ± 7 percent of those computed by the TMB empirical buckling equation.

1. Hemispherical shells (Stiffened)--Collapse--Model tests
2. Hemispherical shells (Stiffened)--Hydrostatic pressure
3. Submarine hulls--Structural analysis
4. Spherical shells (Stiffened)--Design
I. Dadley, Albert E.
II. S-F013 03 02

A nondimensional plot of experimental results is presented for the models tested. Based on the plot, a simple design method is given for similar accurately machined thin spherical shells.

A nondimensional plot of experimental results is presented for the models tested. Based on the plot, a simple design method is given for similar accurately machined thin spherical shells.

A nondimensional plot of experimental results is presented for the models tested. Based on the plot, a simple design method is given for similar accurately machined thin spherical shells.

A nondimensional plot of experimental results is presented for the models tested. Based on the plot, a simple design method is given for similar accurately machined thin spherical shells.

David Taylor Model Basin. Report 1854.
TESTS OF MACHINED HIGH-STRENGTH STEEL SPHERICAL SHELLS SUBJECTED TO EXTERNAL HYDROSTATIC PRESSURE, by Albert E. Dadley. Aug 1964. ii, 21p. illus., tables, graphs, refs. UNCLASSIFIED

Six structural models, consisting of hemispherical shells bounded by ring-stiffened cylinders designed to provide ideal boundary conditions, were hydrostatically pressure tested to collapse. The models were accurately machined from high-strength steel (STS), and were designed to investigate both elastic and inelastic buckling modes of collapse. The results of the tests are compared with the theory and the collapse pressures agree within ± 7 percent of those computed by the TMB empirical buckling equation.

1. Hemispherical shells (Stiffened)--Collapse--Model tests
2. Hemispherical shells (Stiffened)--Hydrostatic pressure
3. Submarine hulls--Structural analysis
4. Spherical shells (Stiffened)--Design
I. Dadley, Albert E.
II. S-F013 03 02

David Taylor Model Basin. Report 1854.
TESTS OF MACHINED HIGH-STRENGTH STEEL SPHERICAL SHELLS SUBJECTED TO EXTERNAL HYDROSTATIC PRESSURE, by Albert E. Dadley. Aug 1964. ii, 21p. illus., tables, graphs, refs. UNCLASSIFIED

Six structural models, consisting of hemispherical shells bounded by ring-stiffened cylinders designed to provide ideal boundary conditions, were hydrostatically pressure tested to collapse. The models were accurately machined from high-strength steel (STS), and were designed to investigate both elastic and inelastic buckling modes of collapse. The results of the tests are compared with the theory and the collapse pressures agree within ± 7 percent of those computed by the TMB empirical buckling equation.

1. Hemispherical shells (Stiffened)--Collapse--Model tests
2. Hemispherical shells (Stiffened)--Hydrostatic pressure
3. Submarine hulls--Structural analysis
4. Spherical shells (Stiffened)--Design
I. Dadley, Albert E.
II. S-F013 03 02

David Taylor Model Basin. Report 1854.
TESTS OF MACHINED HIGH-STRENGTH STEEL SPHERICAL SHELLS SUBJECTED TO EXTERNAL HYDROSTATIC PRESSURE, by Albert E. Dadley. Aug 1964. ii, 21p. illus., tables, graphs, refs. UNCLASSIFIED

Six structural models, consisting of hemispherical shells bounded by ring-stiffened cylinders designed to provide ideal boundary conditions, were hydrostatically pressure tested to collapse. The models were accurately machined from high-strength steel (STS), and were designed to investigate both elastic and inelastic buckling modes of collapse. The results of the tests are compared with the theory and the collapse pressures agree within ± 7 percent of those computed by the TMB empirical buckling equation.

1. Hemispherical shells (Stiffened)--Collapse--Model tests
2. Hemispherical shells (Stiffened)--Hydrostatic pressure
3. Submarine hulls--Structural analysis
4. Spherical shells (Stiffened)--Design
I. Dadley, Albert E.
II. S-F013 03 02

A nondimensional plot of experimental results is presented for the models tested. Based on the plot, a simple design method is given for similar accurately machined thin spherical shells.

A nondimensional plot of experimental results is presented for the models tested. Based on the plot, a simple design method is given for similar accurately machined thin spherical shells.

A nondimensional plot of experimental results is presented for the models tested. Based on the plot, a simple design method is given for similar accurately machined thin spherical shells.

A nondimensional plot of experimental results is presented for the models tested. Based on the plot, a simple design method is given for similar accurately machined thin spherical shells.